

PAPER • OPEN ACCESS

## Taguchi analysis on finite element results to identify the most influential parameters on stresses after impact-damage

To cite this article: E V Arcieri and S Baragetti 2024 *IOP Conf. Ser.: Mater. Sci. Eng.* **1306** 012008

View the [article online](#) for updates and enhancements.

You may also like

- [Detecting the meteoroid by measuring the electromagnetic waves excited by the collision between the hypervelocity meteoroid and spacecraft](#)  
Bo LIU, , Heng ZHANG et al.
- [Dynamic characteristics and crack evolution laws of coal and rock under split Hopkinson pressure bar impact loading](#)  
Xiaoyuan Sun, Tingxu Jin, Jihui Li et al.
- [Self-healing sandwich structures incorporating an interfacial layer with vascular network](#)  
Chunlin Chen, Kara Peters and Yulong Li



**ECS**  
The  
Electrochemical  
Society  
Advancing solid state &  
electrochemical science & technology

**DISCOVER**  
how sustainability  
intersects with  
electrochemistry & solid  
state science research

# Taguchi analysis on finite element results to identify the most influential parameters on stresses after impact-damage

E V Arcieri<sup>1</sup> and S Baragetti<sup>1</sup>

<sup>1</sup>Department of Management, Information and Production Engineering, University of Bergamo, Viale Marconi 5, Dalmine 24044, Italy

emanuelevincenzo.arcieri@unibg.it

**Abstract.** Impact-damage can reduce the fatigue life of mechanical components as a consequence of premature crack growth due to the occurrence of high residual stresses. In this work, finite element analyses were conducted to evaluate the residual stresses in a 7075-T6 aluminium hourglass specimen for various impact cases. The Taguchi method was applied to the finite element results to identify which parameters most influence the residual stresses in the specimen. The outcomes showed that the impact speed is the most influential factor for axial stresses, followed by the material and the size of the impacting object. The factor that most affects the von Mises stresses is the object size followed by its material and the impact speed.

## 1. Introduction

Impact-damage is one of the possible causes of failure of mechanical components, especially in the aeronautical sector [1]. For this reason, this phenomenon represents a hot topic for the scientific community.

Ding et al. [2] identified the occurrence of microcracks and residual stresses as the principal causes of reduction in fatigue strength of components subjected to impact-damage. According to Peters and Ritchie [3], stress risers in the damaged area induce early failure of components hit by foreign bodies. Boyce et al. [4] performed numerical calculations to determine the residual stresses and damage induced by a body impacting a plate. The results showed that for low-speed impacts quasi-static numerical analyses ignoring material strain-rate sensitivity, wave, and inertia effects are adequate, but dynamic simulations are required for severe impact loading. According to Martinez and colleagues [5], the principal reasons for failure in components with impact-damage are post-impact stress risers and residual stresses. Nowell et al. [6] found that the depth of the impact-induced dent has a significant impact on fatigue strength. The consequences of the notch presence are nonetheless mitigated by a compressive stress condition seen near its root. In a numerical analysis of the damage resulting from a ball striking the edge of a thin plate, Chen [7] found that a static stress concentration factor smaller than 1 occurs at the bulge tip while the concentration factor was higher than 1 at the base of the impact-generated dent. In order to assess the impact of residual stresses, Ruschau et al. [8] conducted a stress relief annealing after impact-damage. The stress relief was unsuccessful in improving the fatigue resistance of specimens damaged at high speeds because of the resulting material loss.

In summary, residual stresses significantly influence the fatigue behavior of impact-damaged components, as also demonstrated in [9,10] for other mechanical situations. This study examines the residual stress distribution induced by the impact-damage in an hourglass specimen made of 7075-T6 aluminium alloy, which is a material commonly used for manufacturing aeronautical components. The



post-impact stresses are modelled with the Abaqus Explicit finite element code. Taguchi analysis was conducted on the finite element results in order to quickly and efficiently identify the parameters that most influence the residual stresses in the specimen.

## 2. Finite element model

The Abaqus Explicit finite element code [11] was used to simulate the impact of the ball on the hourglass specimen, as is commonly done for impact problems, which involve geometric and material nonlinearities [12-16].

The model for the impact simulation is shown in Figure 1 [17-19]. The 7075-T6 specimen was modeled using general purpose linear brick elements with reduced integration and an overall mesh size of 0.25 mm in the impact area. The 7075-T6 specimen was considered to have an isotropic elastic perfectly plastic material behavior, with the properties shown in the figure. Linear quadrilateral rigid elements were used to model the ball, with an overall mesh size of 0.25 mm. The ball inertial properties were assigned to its center, which was positioned on the same plane of the minimum cross-section of the hourglass specimen. The impact ball materials implemented in the finite element analyses are steel and ceramic, with the properties reported in the figure [20]. The tested diameters  $D$  are 5 and 7 mm.

A space of 0.1 mm was left between the specimen outer surface and the ball outer surface. All analyses were run with a friction coefficient of 0.6 [21] between the ball and the hourglass specimen. The surface nodes in the areas of the hourglass specimen marked in Figure 1 were fixed. Normal and inclined impact were analyzed, with impact angles  $\alpha=0^\circ$  or  $\alpha=20^\circ$  and  $\beta=0^\circ$  or  $\beta=20^\circ$ . The angle  $\alpha$  is measured on the plane  $xz$  and  $\beta$  on the plane  $yz$  (Figure 1). The tested initial ball speeds  $v$  are 80 m/s or 120 m/s. The stress state used for the Taguchi analysis is that obtained after a simulated time of 7 ms from the beginning of the movement of the sphere, when the stresses can be considered constant in the specimen over time.

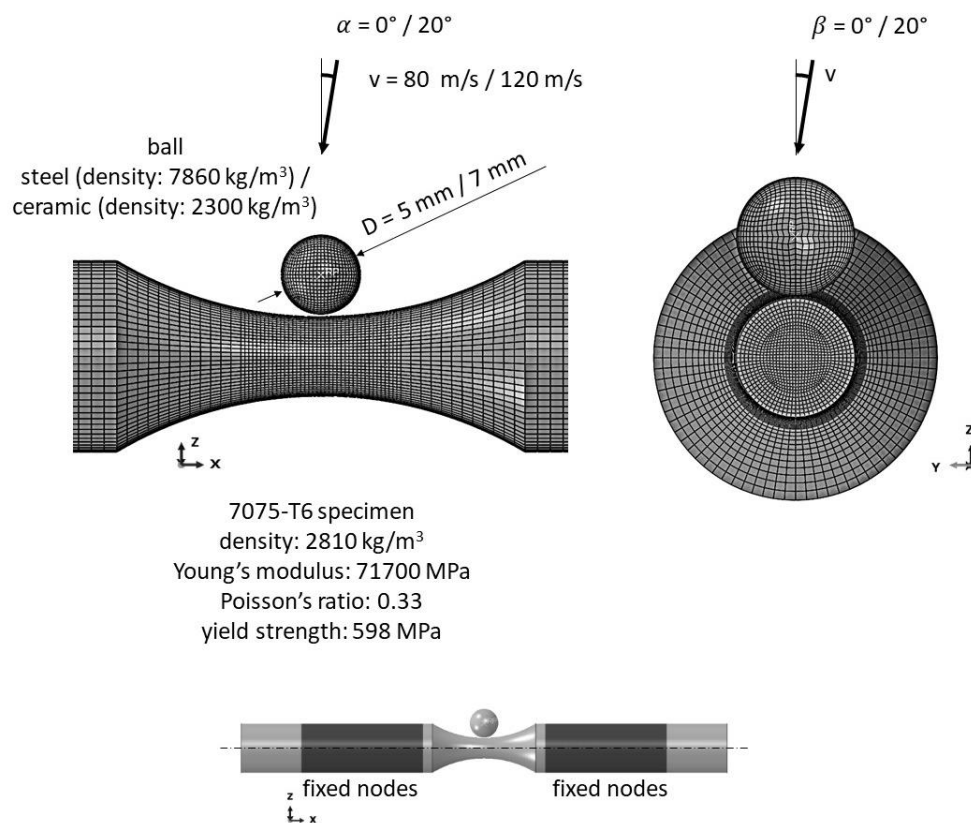


**Figure 1.** Finite element model [17-19].

### 3. Taguchi analysis on axial stresses

The most significant factors for impact-damage were identified thanks to the Taguchi analysis [22]. Fatigue cracks may propagate from the locations of high tensile stresses and therefore the Taguchi method was used to determine which factors most generate high residual stresses in the specimen. The Taguchi L8(2<sup>7</sup>) array was used, which requires only eight runs to examine the influence of seven factors with two levels. Table 1 contains the array including the parameters and their corresponding levels [17,20]. The impact speed,  $v$ , the ball material, Material, the ball diameter,  $D$ , the impact angles,  $\alpha$  and  $\beta$ , are the elements taken into consideration in the study. It was possible to check if all the parameters that significantly influence the residual stresses were considered by introducing the empty columns e1 and e2.

**Table 1.** Taguchi L8(2<sup>7</sup>) array employed for the study [17,20].

Run	$v$ (m/s)	Material	$D$ (mm)	$\alpha$ (°)	$\beta$ (°)	e1	e2
1	80	Steel	5	0	0	1	1
2	80	Steel	5	20	20	2	2
3	80	Ceramic	7	0	0	2	2
4	80	Ceramic	7	20	20	1	1
5	120	Steel	7	0	20	1	2
6	120	Steel	7	20	0	2	1
7	120	Ceramic	5	0	20	2	1
8	120	Ceramic	5	20	0	1	2

After impact, it was supposed that the specimen was exposed to axial or bending cyclic loading. Since both loading conditions produce a variable axial stress distribution, the axial residual stresses were analyzed [17].

Figure 2 shows the distributions of the axial stress, S11, obtained at the end of the eight simulations. The Taguchi analysis was conducted on the maximum axial stress in the specimen. Table 2 is the 'Response table' and was constructed with the results of Figure 2 according to the methodology reported in [22]. The column Y of the table reports the maximum axial residual stress in each run. Low tensile residual stresses are preferable from a fatigue point of view. For this reason, the analysis was conducted according to the modality 'smaller is better' and the mean square deviation MSD was calculated as  $MSD = \sum Y^2 / n$ , with the number of simulations per run,  $n$ , equal to 1 due to the deterministic nature of the results. The subsequent steps in the Taguchi method consist in the calculation of  $S/N = -10 \log(MSD)$ , of  $Y'$  and of  $S/N'$ , where  $S/N$  is the signal-to-noise ratio,  $Y'$  is the average of the stresses obtained in the runs in which the factor  $x$  is at level  $y$  and  $S/N'$  is the average of the  $S/N$  values obtained when a considered factor  $x$  is at a considered level  $y$ . The quantity  $\Delta S/N'$  represents the difference between the  $S/N'$  calculations for the two levels of the parameter taken into account. The significance of a parameter is higher than that of another if its  $\Delta S/N'$  value is greater [22]. The impact velocity  $v$  ( $\Delta S/N' = 2.804$ ) is the most influential factor, followed by the material ( $\Delta S/N' = 2.723$ ) and the diameter  $D$  ( $\Delta S/N' = 2.630$ ) of the ball. The values of  $\Delta S/N'$  for the other factors are very small compared to those of  $v$ , Material and  $D$ . Therefore, the influence of the other parameters on the axial stresses in the specimen is very low. The analysis of the empty columns reveals that no significant factors were neglected.

The level of the important parameters which allows to minimize the stresses in the specimens corresponds to the highest  $S/N'$  [22]. Low impact speed, low material density and small size of the impacting objects induce low axial stresses.

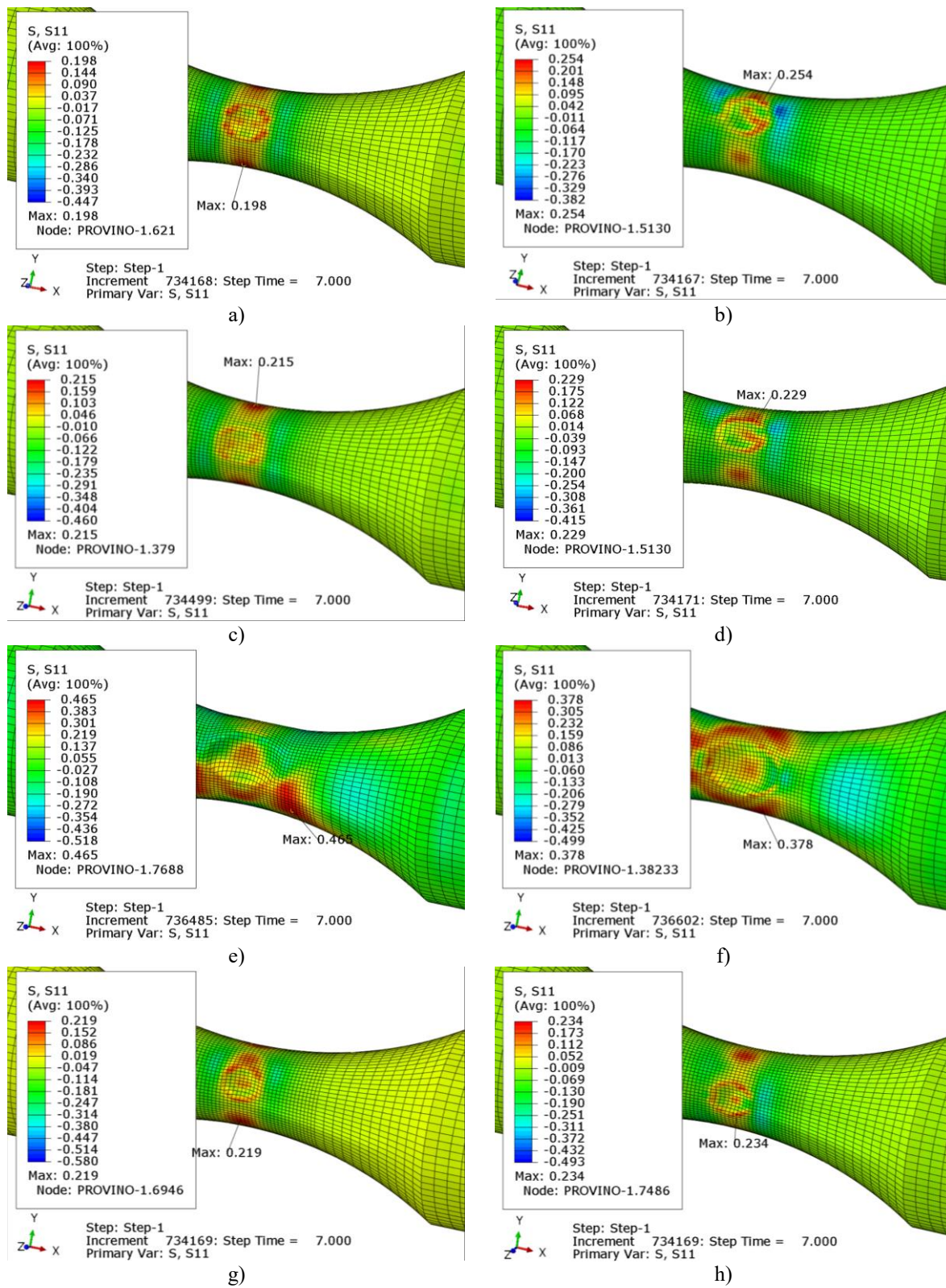


**Figure 2.** Axial stresses (GPa): a) Run1, b) Run 2, c) Run 3, d) Run 4, e) Run 5, f) Run 6, g) Run 7, h) Run 8 [17].

**Table 2.** Response table for maximum axial stress [17].

Run	Y	MSD	S/N	Factor	Level	Y'	S/N'	$\Delta S/N'$
1	198	39204	-45.933	v (m/s)	80 m/s	224	-46.969	2.804
2	254	64516	-48.097		120 m/s	324	-49.773	
3	215	46225	-46.649	Material	steel	324	-49.732	2.723
4	229	52441	-47.197		ceramic	224	-47.010	
5	465	216225	-53.349	D (mm)	5	226	-47.056	2.630
6	378	142884	-51.550		7	322	-49.686	
7	219	47961	-46.809	$\alpha$ (°)	0	274	-48.185	0.372
8	234	54756	-47.384		20	274	-48.557	
				$\beta$ (°)	0	256	-47.879	0.984
					20	292	-48.863	
				e1	1	282	-48.466	0.190
					2	267	-48.276	
				e2	1	256	-47.872	0.998
					2	292	-48.870	

#### 4. Taguchi analysis on von Mises stresses

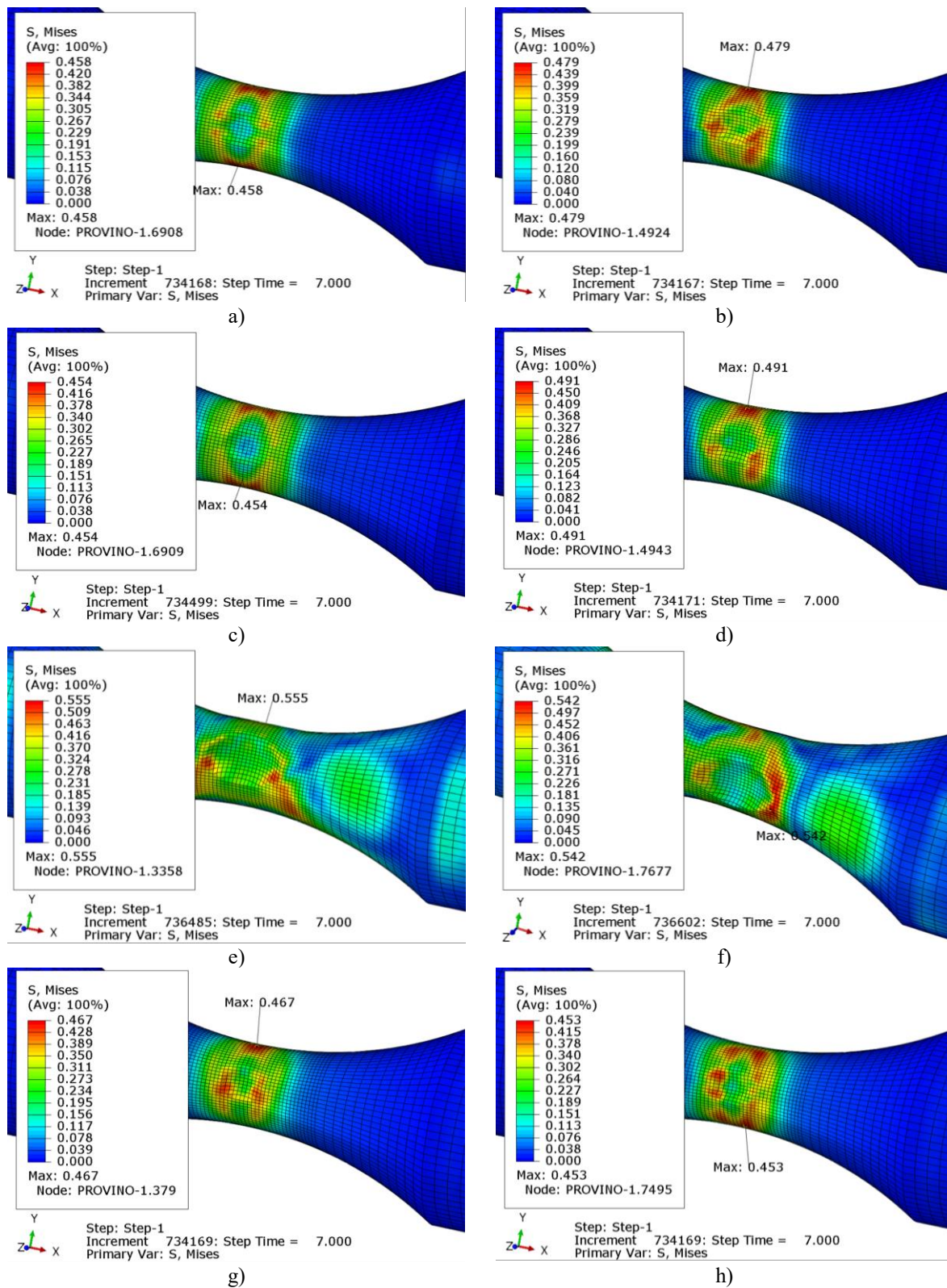
In order to evaluate the complexity of the stress field induced by the impact, the Taguchi method was also applied to identify the factors that mostly influence von Mises stresses in the specimen.

Figure 3 shows the von Mises stress distributions at the end of the eight runs. The Taguchi analysis was conducted on the maximum axial von Mises stress in the specimen. Table 3 is the 'Response table' for maximum von Mises stress. Column Y of the table reports the maximum von Mises stress after each simulated impact. The Taguchi analysis was again conducted according to the modality 'smaller is better'. Even if all the values of  $\Delta S/N'$  are very small, it can be stated that the impact parameter which most influences the von Mises stresses in the specimen is the diameter D of the ball ( $\Delta S/N'=0.799$ ), followed by the material of the impacting object ( $\Delta S/N'=0.730$ ) and the impact speed v ( $\Delta S/N'=0.572$ ). The  $\Delta S/N'$  values of the other factors are smaller and therefore their influence on the von Mises stresses is very low. The analysis of the empty columns points out that no significant factors were ignored.

Looking at the S/N' values, low impact speed, low material density and small size of the impacting objects induce low von Mises stresses.

#### 5. Discussion

In both the analyses on axial and von Mises stress, it was found that the diameter and the material of the ball and the impact speed are the most influential parameters and that low values of these quantities induce low residual stresses. The density and size of the impacting object influence its mass, which multiplied by the impact speed gives its initial momentum. A high momentum means a high impact force and therefore high deformations and stresses in the impacted object. However, the order of parameter importance is different. Impact velocity is the most significant factor for axial stresses, followed by ball material and diameter. The impact parameter that most influences the von Mises stresses in the specimen is the diameter of the ball followed by its material and the impact speed.



**Figure 3.** Von Mises stresses (GPa): a) Run1, b) Run 2, c) Run 3, d) Run 4, e) Run 5, f) Run 6, g) Run 7, h) Run 8.

**Table 3.** Response table for maximum von Mises stress.

Run	Y	MSD	S/N	Factor	Level	Y'	S/N'	$\Delta S/N'$
1	458	209764	-53.217	v (m/s)	80 m/s	471	-53.447	0.572
2	479	229441	-53.607		120 m/s	504	-54.019	
3	454	206116	-53.141	Material	steel	509	-54.097	0.730
4	491	241081	-53.822		ceramic	466	-53.368	
5	555	308025	-54.886	D (mm)	5	464	-53.333	0.799
6	542	293764	-54.680		7	511	-54.132	
7	467	218089	-53.386	$\alpha$ (°)	0	484	-53.658	0.150
8	453	205209	-53.122		20	491	-53.808	
				$\beta$ (°)	0	477	-53.540	0.385
					20	498	-53.925	
				e1	1	489	-53.762	0.058
					2	486	-53.704	
				e2	1	490	-53.776	0.087
					2	485	-53.689	

The maximum von Mises stress values obtained in the eight runs are approximately twice the maximum axial stress values. This means that the axial stress distribution could not fully describe the complex stress state in the specimen. This aspect would influence the fatigue behavior of the specimen.

The maximum stress values were analyzed without considering the position in which they occurred. Under fatigue loading, stress concentrations due to impact can induce high total stresses in other positions in the specimen and therefore the contribution of stress risers should be evaluated.

## 6. Conclusions

In this work, the Taguchi method was applied to the finite element results to identify the parameters that most influence the residual stresses in a 7075-T6 specimen subjected to impact-damage. The impact velocity is the factor that most influences axial stresses, followed by the material and the size of the impacting object. The factor that most influences the von Mises stresses in the specimen is the diameter of the object, followed by its material and the impact velocity. The comparison between the von Mises stress and the axial stresses obtained in the eight runs leads to the conclusion that axial stresses could not fully describe the complex stress state in the specimen after impact-damage. Future developments could include the creation of a theoretical model that allows to predict the shape of the damage after impact and the associated stress distribution as done in [23] for another mechanical problem.

## References

- [1] Nicholas T 2006 Foreign Object Damage *High Cycle Fatigue*, Elsevier Science Ltd (Oxford) pp x–xiv
- [2] Ding J, Hall R F, Byrne J and Tong J 2007 *Int. J. Fatigue* **29** 1339
- [3] Peters J O and Ritchie R O 2000 *Eng. Fract. Mech.* **67** 193
- [4] Boyce B L, Chen X, Hutchinson J W and Ritchie R O 2001 *Mech. Mater.* **33** 44
- [5] Martinez C M, Eylon D, Nicholas T, Thompson S R, Ruschau J J, Birkbeck J and Porter W J 2002 *Mat. Sci. Eng.* **A325** 465
- [6] Nowell D, Duó P and Stewart I F 2003 *Int. J. Fatigue* **25** 963
- [7] Chen X 2005 *Mech. Mater.* **37** 447



- [8] Ruschau J, Thompson S R and Nicholas T 2003 *Int. J. Fatigue* **25** 955
- [9] Baragetti S and Tordini F 2007 *Int. J. Fatigue* **29** 1832
- [10] Mlikota M, Schmauder S, Dogahe K and Božić Ž 2021 *Procedia Struct. Integr.* **31** 3
- [11] ABAQUS, ABAQUS Documentation, Dassault Systèmes, Providence, RI, USA, 2017
- [12] Baragetti S, Guagliano M and Vergani L 2000 *Int. J. Mater. Prod. Technol.* **15** 91
- [13] Arcieri E V, Baragetti S, Fustinoni M, Lanzini S and Papalia R 2018 *Procedia Struct. Integr.* **8** 212
- [14] Baragetti S and Arcieri E V 2019 *Procedia Struct. Integr.* **24** 91
- [15] Wang W and Shi J 2013 *Int. J. Impact Eng.* **60** 67
- [16] Baragetti S and Arcieri E V 2020 *Eng. Fail. Anal.* **113** 104564
- [17] Arcieri E V, Baragetti S and Božić Ž 2021 *Procedia Struct. Integr.* **31** 22
- [18] Arcieri E V, Baragetti S and Božić Ž 2022 *Eng. Fail. Anal.* **138** 106380
- [19] Arcieri E V, Baragetti S, Božić Ž 2023 *Procedia Struct. Integr.* **46** 24
- [20] Baragetti S 1997 *Int. J. Mat. Prod. Tech.* **12** 83
- [21] Javadi M and Tajadri M 2013 *Tribol. Ind.* **35** 286
- [22] Condra L W 1993 *Reliability improvement with Design of Experiments* Marcel Dekker Inc (New York)
- [23] Baragetti S 2006 *Meccanica* **41** 443